GEOMETRIC INTERPRETATION OF DUAL-POLARIZATION RADAR METEOROLOGICAL OBSERVATIONS

Paul Krehbiel and Richard Scott

Langmuir Laboratory, New Mexico Tech, and National Radio Astronomy Observatory

Socorro, New Mexico, 87801

The polarization state of electromagnetic radiation is completely characterized by four quantities related to the signal *powers* in orthogonal polarizations. Examples are the Stokes parameters Q,U,V and I, or, equivalently, the measured covariances W_1 and W_2 of the signals in two orthogonal polarizations and the magnitude and phase of the complex cross-covariance W between the two signals. Stokes parameters Q,U,V describe the polarized part of the signal and correspond to the Cartesian coordinates of the polarization state on the surface of the Poincaré sphere (Figure 1). Each parameter corresponds to linear power *differences* in the three dimensional Poincaré space, with $Q = W_H - W_V$, $U = W_+ - W_-$, and $V = W_L - W_R$. The total polarized power is the Pythagorean sum $I_p = \sqrt{Q^2 + U^2 + V^2}$ and corresponds to the radius of the Poincaré sphere. The fourth Stokes parameter, I, is the total power of signal, namely the sum of the polarized and unpolarized signal components $I = I_p + I_{unpolarized}$. It accounts for the presence of an unpolarized component. The linear relation between the Stokes parameters and the polarization powers implies that superposition applies in Poincaré space, which is important in interpreting dual-polarization radar observations.
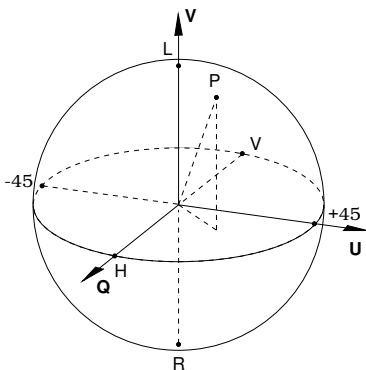

Figure 1. The Poincaré sphere representation of the polarization state.

For meteorological radars, the scattered signal from a given volume of particles in range has an average power that is the sum (i.e., superposition) of the powers from each individual scatterer. This is an unusual property of signals - normally power values do not superimpose. It results from the particles being randomly distributed in range and constantly rearranging, so that the scattering is uncorrelated from one particle to the next. The important implication for dual-polarization radar measurements is that the polarization effects produced by the scatterers are also additive, and superimpose in Poincaré space. The overall polarization state of radar signals is therefore the superposition of the polarization effects of different types or classes of particles.

An important issue of dual-polarization meteorological observations is that the reflected signal has an unpolarized component, in addition to the polarized component. The unpolarized component results from any variations or randomness in the scatterers, such as their size, shape and/or orientation, and is highly useful in remotely sensing the presence of randomness such as that associated with graupel and hail. At the same time the effect of the unpolarized component needs to be taken into account in evaluating polarization observations. In terms of the Stokes/Poincaré representations, for a given total reflected power I the effect of some of the power being unpolarized is to reduce the radius of the Poincaré sphere by the fractional degree of polarization, $p = I_p/I$.

It is interesting to note that the instantaneous return from a given arrangement of scatterers is completely polarized, in that the two polarization signals each consist of a sinusoid at the radar frequency f_0, having some amplitude A and phase ϕ. If the particles were frozen in place relative to one another, the phasor $Ae^{j\phi}$ would rotate uniformly at a rate corresonding to the Doppler velocity of the particle assemblage. The polarization state for a fixed arrangement of particles would be incompletely determined and would have no unpolarized component. The fact that the scatterers rearrange from one transmitted pulse to the next causes the $A-\phi$ phasor to rotate in a fluctuating manner about the mean Doppler rate, thereby enabling the average power to be determined and also giving rise to an unpolarized component.

For interpreting dual-polarization observations, it is useful conceptually to categorize the particles into several basic types or classes based on their polarization effects: a) spherical particles, which do not depolarize, b) oriented or aligned particles, which have differential reflectivity, differential phase, and correlation effects, and c) randomly shaped and/or oriented particles, which primarily introduce an unpolarized component that further reduces the correlation. The various effects combine additively power-wise in Poincaré space to give polarization 'trajectories' along radial beams through a storm, that can be visualized geometrically and conceptually in the 3-dimensional Poincaré space (e.g., Figs. 7 and 8).

The above categorization of particle types results from different symmetries in their polarization effects. For horizontally oriented particles such as liquid drops, the polar-

ization changes are rotationally symmetric about the Q or H,V axis of the Poincaré sphere. The effects are therefore best measured in an H,V polarization basis and are most naturally described in a spherical coordinate system in Poincaré space, with the +Q or positive H,V Stokes axis being the polar axis. Defining the polar angle to be 2α, as in Figure 2, the effect of differential reflectivity Z_{DR} is to increase the horizontal power W_H relative to the vertical power W_V, thereby causing Q to increase and the polarization state to move toward the H polarization point by decreasing 2α. Differential attenuation has the opposite effect of reducing the horizontal power relative to the vertical, causing the polar angle to increase toward the V polarization point on the back side of the sphere. The azimuthal angle ϕ corresponds to the phase difference between the H and V components and is therefore changed by differential propagation phase ϕ_{dp} and differential backscatter δ_ℓ. Finally, the radial component of the polarization state is reduced by the degree of polarization p, which is determined from the ρ_{HV} correlation coefficient of the covariance measurements, termed 'f'. The above changes are in orthogonal or nearly orthogonal directions in Poincaré space when equal- or nearly equal-power H and V polarizations are transmitted simultaneously, either as slant $45°$ linear or circular polarization.
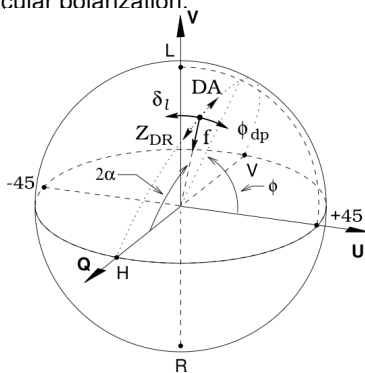

Figure 2. The effect of scattering by horizontally oriented particles, which is rotationally symmetric about the Q or H,V axis.
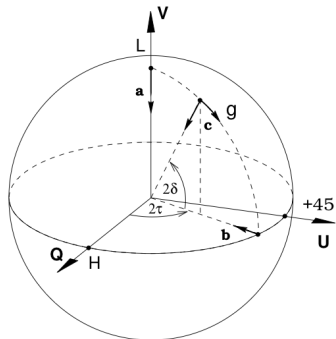

Figure 3. The effect of scattering by randomly oriented particles, which is rotationally symmetric about the V or LHC/RHC axis.

By contrast, the polarization effects of randomly oriented or shaped particles, such as hail, are symmetric about the vertical Poincaré axis, namely V or LHC,RHC circular polarization axis of the Poincaré sphere (Figure 3). The effects are therefore best described in an LHC,RHC

basis, and also in a spherical coordinate system in which the polar axis is now the upward V axis. The scattering reduces both the degree of polarization p and makes the polarization state more linear by moving it toward the linear polarization equator. Whereas the polarization effects of aligned particle scattering is characterized by 4 parameters (Z_V, Z_{DR}, ρ_{HV}, and ϕ_{dp}), random scattering is characterized by only two parameters - the average reflectivity S_{avg} and a quantity g, termed the sphericity parameter,

$$ g = \frac{4\text{Re}\{\langle S_{xx}S_{yy}^*\rangle\}}{\langle|S_{xx}+S_{yy}|^2\rangle} , \qquad (1) $$

(Scott, 1999; Scott et. al., 2001). The polarization state itself is affected only by g, which measures the departure of the particle shapes from spherical. g is unity for spherical particles and decreases to zero for increasingly elliptical or variable shapes. Therefore, $0 \le g \le 1$. An important result is that the reduction in the degree of polarization is a factor of two or more for circular polarization than for linear. This results from the fact that circularly polarization is equally depolarized by particles of all orientation, while linear polarization is not depolarized by particles that are aligned or close to being aligned with the incident linear radiation.
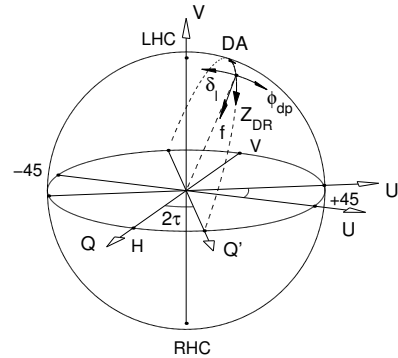

Figure 4. The rotated polarization changes produced by particles oriented at an angle τ relative to horizontal.

For particles that are oriented in non-horizontal directions, such as electrically aligned ice particles, the polarization changes are symmetric about a Q' axis that is rotated in the equatorial or azimuthal plane of the Poincaré sphere. Denoting the orientation angle from horizontal by τ, the azimuthal rotation is 2τ. For particles oriented at $\pm 45°$, the rotation angle is 90 degrees, and differential propagation phase of electrically aligned particles will appear as a positive or negative Z_{DR} value. This highlights the fact that processing dual polarization data in one basis gives incorrect results when the depolarization is in a different basis. This is not the case for degree of polarization measurements, as p is independent of the basis in which it is calculated.

Polarization trajectories Figures 5 and 6 show examples of polarization trajectories through mixed rain and hail (Fig. 5) and through an electrical alignment region in the upper part of a storm (Fig. 6), from Scott et al. (2001).
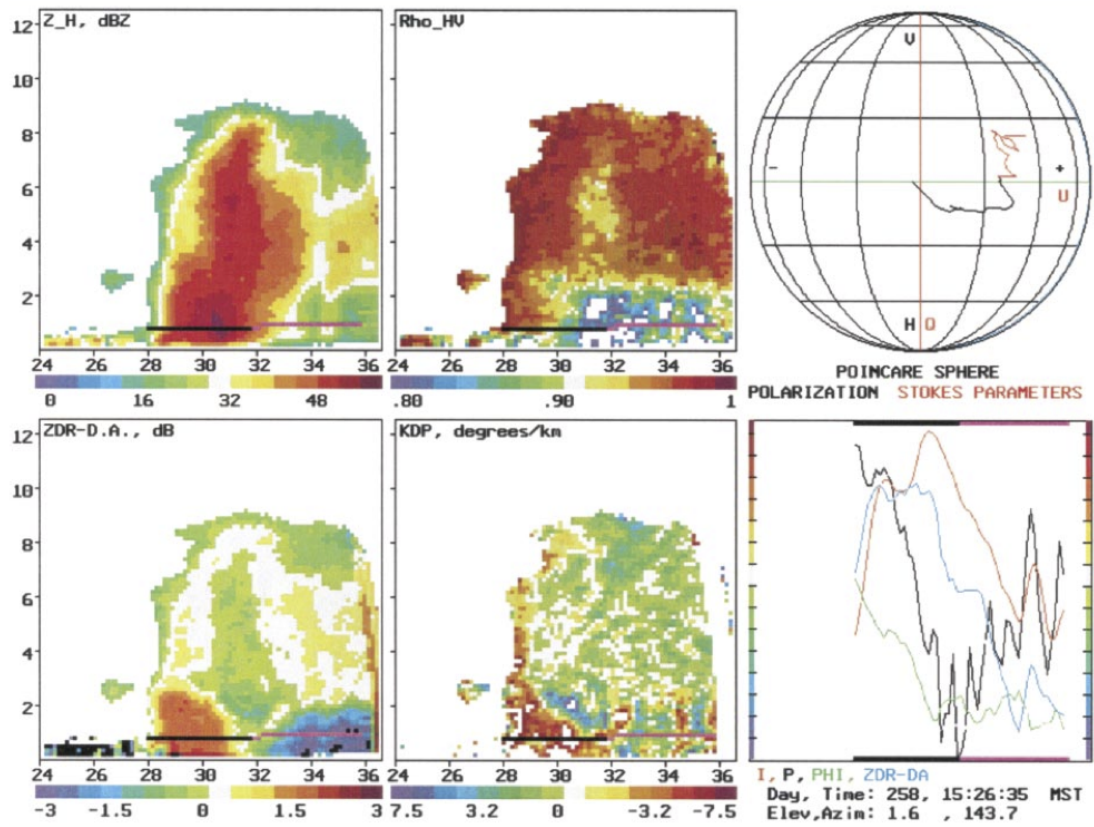
Figure 5. Polarization variables and example trajectory through mixed rain and hail in a storm on September 15, 1998.
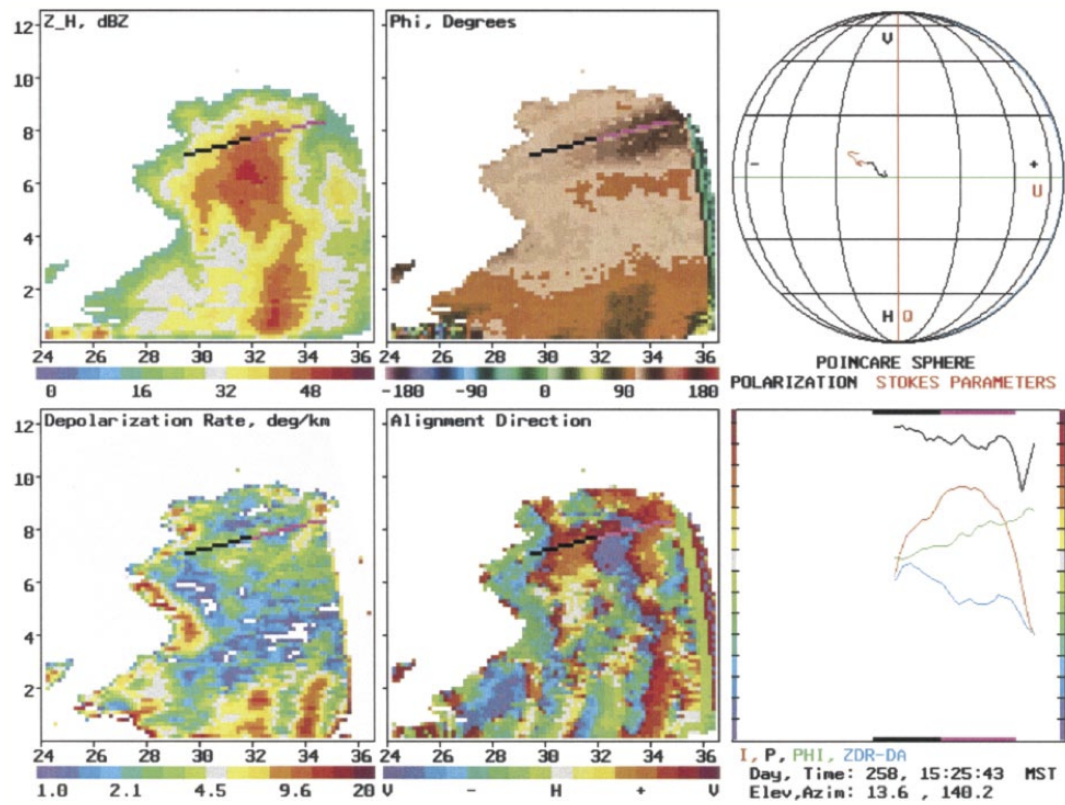

Figure 6. Same as Figure 5, except showing a trajectory through an electrical alignment region in the upper part of the storm.
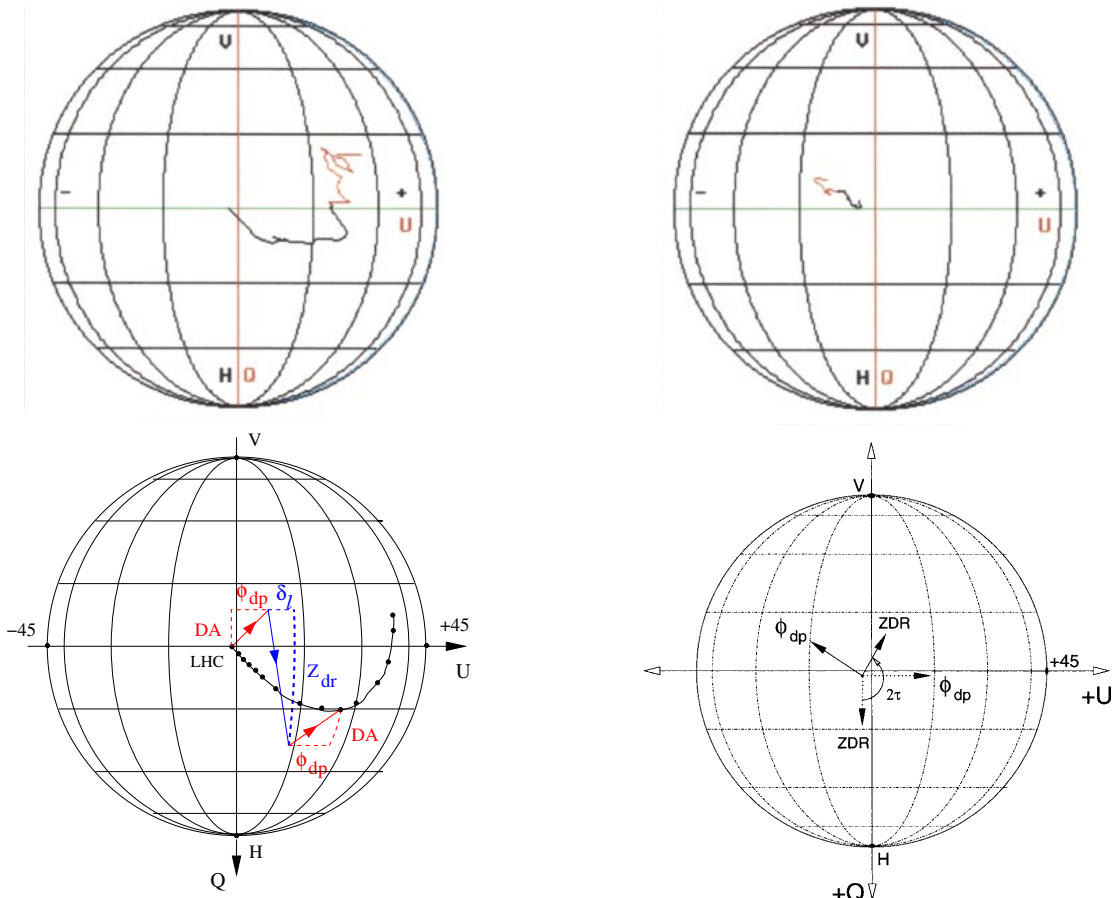
Figure 7. Top: Expanded view of the polarization trajectory of Fig. 5. Bottom: Conceptual illustration of how the polarization state at a given range gate is arrived at from the cumulative propagation effects of differential attenuation (DA) and phase (ϕ_{dp}) (red), and the backscatter effects of differential phase (δ_ℓ) and reflectivity Z_{DR} (blue).

Figure 8. Top: Expanded view of the polarization trajectory of Fig. 6. Bottom: Illustration of how non-horizontal alignment changes the directions of ϕ_{dp} and Z_{DR} effects. Normal H,V processing interprets the changes as if they were produced by horizontally oriented particles (dotted arrows), and misinterprets the change as being due to negative Z_{DR} and negative ϕ_{dp} values.

The trajectories are shown as viewed from above the Poincaré sphere and show how the Stokes parameters Q and U change with range. In both figures the trajectories begin near the circular polarization point in the center of the projection, corresponding to LHC transmitted polarization. An expanded view of the trajectory for the mixed rain/hail observation is shown in Figure 7. The trajectory initially developed downward and to the right as a result of the combined effects of Z_{DR} and ϕ_{dp} upon entering the rain region, then to the right as a result of steadily increasing ϕ_{dp}. The effects of Z_{DR} and differential attenuation appear to remain constant during the latter range interval. Upon leaving the strong rain region, ϕ_{dp} stops increasing and Z_{DR} gradually decreases, moving the trajectory upward toward the V polarization point and revealing the cumulative effect of differential attenuation.

The bottom panel of Figure 7 illustrates conceptually how the polarization state at a given range gate is reached. The red vectors show the cumulative propagation effects of differential attenuation and phase, both before and after backscatter, while the blue vector shows the effect of

differential phase upon backscatter and differential reflectivity. A side view from in front of the Poincaré sphere would show how the degree of polarization changes due to variability in particle shapes and random particle orientations. Both views would show the polarization observations in Cartesian coordinates, for which superposition holds. The trajectory of Fig. 7 is thus the superposition of those for the horizontally oriented rain and randomly shaped and oriented hail. Because of this it should be possible in principle to decompose the two contributions with appropriate polarization-diverse measurements.

The polarization trajectory for the electrical alignment observations (Figure 8) exhibits a different behavior, developing upward and to the left with increasing range, that is sustained until the radar beam exited the storm. For the expected case in which the depolarization by aligned ice crystals is due primarily to ϕ_{dp} and not to Z_{DR} effects, the orientation of the trajectory is indicative of the alignment direction, as in the bottom part of Fig. 8. However, the H,V processing interprets the trajectory as a combination

of negative ϕ_{dp} and negative Z_{DR} values that continually increase with range, producing radial 'striping' characteristic of a propagation effect. The correct interpretation is that the trajectory is due to the differential propagation phase of the aligned ice particles in the rotated polarization basis corresponding to the alignment direction. Because the electric fields in thunderstorms are predominantly vertical, the alignment directions are also vertical, so that electrical alignment is usually detected by negative ϕ_{dp} stripes, as in the upper middle panel of Fig. 6. However, when tilted from vertical, as around the periphery of charge regions, the alignment is interpreted as negative or positive Z_{DR} values and detected from Z_{DR} striping in Z_{DR}.

Figure 9 shows an example of Z_{DR} striping in the uppermost part of the storm of Fig. 5. In this case the apparent Z_{DR} values are positive, indicative of $-45°$ alignment. The polarization trajectory of such alignment would be downward directed in the projection plane plots.
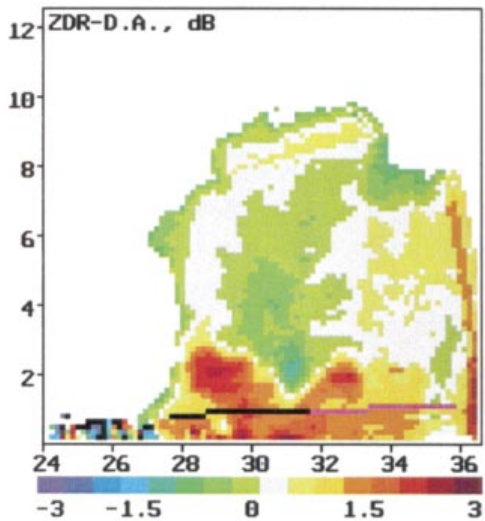

Figure 9. Positive Z_{DR} stripe in the upper part of the storm of Fig. 5, 3.5 min earlier in time, indicative of a significant $-45°$ component of electrical alignment. From Fig. 4 of Scott et al., 2001.

Understanding and interpreting electrical alignment observations is a particular example of the utility of the geometric Poincaré approach. Analysis of non-horizontal alignment in an H,V basis is extremely tedious (e.g., Ryzhkov and Zrnic, 2007), but is simple in the Poincaré approach. The polarization effects are identical to those of horizontally aligned particles, except about a rotated axis of symmetry in the equatorial plane of the Poincaré sphere. The electrical alignment case illustrates the difficulty of interpreting observations in a different basis than the natural basis of the polarization effects.

Details and quantitative analyses of the Poincaré approach have been developed by Scott (1999), Scott et al., (2001), and Krehbiel and Scott (in preparation). Results from these early studies were also presented at the 30th Radar Meteorology Conference in Munich (Scott et al., 2001a,b).

Effect of unpolarized components. The Poincaré formulations enable the various polarization effects to be conceptualized and visualized geometrically, which substantially aids in their understanding and interpretation. In this section we use the formulations to discuss the effect of an unpolarized component on radar observations.

The Poincaré formulations are straightforwardly derived from the covariances of signals in a set of two orthogonal polarizations (e.g., Born and Wolf, 1999). In particular, the signal scattered back to the radar from a given volume in range will in general have a polarized component and an unpolarized component, and can be represented by its complex amplitudes in two orthogonal polarizations:

$$\hat{E}_1 = E_1 e^{j\phi_1} + \hat{E}_{u1}(t)$$
$$\hat{E}_2 = E_2 e^{j\phi_2} + \hat{E}_{u2}(t) \ . \tag{2}$$

The first term on the right hand side of each expression is the complex amplitude of the polarized component and the second term is the complex amplitude of the unpolarized component, which by definition is time-varying. For a given arrangement of scatterers, the polarized component has well-defined amplitudes and phases that describe the polarization ellipse. The amplitudes and phases of the unpolarized component vary randomly with time and are uncorrelated with the polarized components and with each other.

The radar antenna and receiving system sense the complex amplitudes of the two polarizations and provide estimates of the covariances

$$W_1 = \langle \hat{E}_1 \hat{E}_1^* \rangle = E_1^2 + E_u^2$$
$$W_2 = \langle \hat{E}_2 \hat{E}_2^* \rangle = E_2^2 + E_u^2 \tag{3}$$
$$W = \langle \hat{E}_1 \hat{E}_2^* \rangle = E_1 E_2 \, e^{j(\phi_1 - \phi_2)} = |W| e^{j\phi} \ .$$

where E_1^2 and E_2^2 are the powers of the polarized components and $E_u^2 \equiv \langle |\hat{E}_{u1}|^2 \rangle = \langle |\hat{E}_{u2}|^2 \rangle$ is the power of the unpolarized component, which is equal in the two polarizations. The angle $\phi = (\phi_1 - \phi_2)$ is the phase difference between the polarized component in the two polarizations. The effect of receiver noise will be to add uncorrelated signals to each channel and has the same effect as an unpolarized component.

The covariances can be written in matrix form, called the coherency matrix J (e.g., Born and Wolf, p. 620–627, 1975; Mott, 1986; Bringi and Chandrasekhar, p. 127, 2001). J is defined as below and can be decomposed into unpolarized and polarized components according to

$$J = \begin{bmatrix} W_1 & W \\ W^* & W_2 \end{bmatrix} = \begin{bmatrix} A & 0 \\ 0 & A \end{bmatrix} + \begin{bmatrix} B & D \\ D^* & C \end{bmatrix} \ . \tag{4}$$

From (3), the elements of the fully polarized matrix are $B = E_1^2$, $C = E_2^2$, and $D = E_1 E_2 e^{j\phi}$. For the unpolarized matrix, $A = E_u^2$. The polarized matrix has the property that its determinant is zero, or $BC = |D|^2$.

The covariances determine four quantities: W_1, W_2, and $|W|$ and $\angle W = \phi$ (or, equivalently, $\text{Re}[W]$ and $\text{Im}[W]$). The decomposed covariance matrices (4) are described by five quantities (A, B, C, $|D|$, and $\angle D$), whose values can be obtained from the covariances and from the polarization constraint $BC = |D|^2$. In particular,

$$2A = (W_1 + W_2) - \sqrt{(W_1 - W_2)^2 + 4|W|^2}$$

$$2B = (W_1 - W_2) + \sqrt{(W_1 - W_2)^2 + 4|W|^2}$$

$$2C = (W_2 - W_1) + \sqrt{(W_1 - W_2)^2 + 4|W|^2}$$

$$D = W . \tag{5}$$

The decomposed quantities involve only the sum and difference of W_1 and W_2 and not W_1 or W_2 individually. Furthermore, the polarized quantities B and C involve only the difference term, $(W_1 - W_2)$. The result that $D = W$ is seen by inspection of (4) and follows from the fact that the cross-covariance W is unaffected by the presence of an unpolarized component (or by receiver noise).

The above quantities have the interpretation that $(W_1 + W_2)$ is the total signal power I, $(B + C)$ is the total polarized power I_p, and $2A$ is the total unpolarized power, which is equally split between the two polarizations. $(W_1 - W_2)$ is the difference of the orthogonal powers in the measurement basis and corresponds to the Stokes parameter in that basis. From (5), the total polarized power $(B + C)$ is given by

$$B + C = \sqrt{(W_1 - W_2)^2 + 4|W|^2} = I_p . \tag{6}$$

This expresses the polarized power in terms of the power difference $(W_1 - W_2)$ and is a fundamental result for deriving the Poincaré and Stokes results. In particular, since

$$\hat{W} = |W|e^{j\phi} = |W|\cos\phi + j|W|\sin\phi \tag{7}$$

one has that $4|W|^2 = (2|W|\cos\phi)^2 + (2|W|\sin\phi)^2$. Thus, the expression for the polarized power becomes

$$B + C = \sqrt{(W_1 - W_2)^2 + (2|W|\cos\phi)^2 + (2|W|\sin\phi)^2}$$
$$\equiv I_p . \tag{8}$$

The total polarized power is therefore the sum of three orthogonal quantities: $(W_1 - W_2)$, $2|W|\cos\phi$, and $2|W|\sin\phi$. The Pythagorean nature of this result is readily apparent and can be illustrated graphically. As noted earlier, the $(W_1 - W_2)$ axis corresponds to the Stokes parameter in the measurement basis. For the case in which the measurements are in an H–V basis, $W_1 - W_2 = W_H - W_V$, which is the Stokes parameter Q. Similarly, the cross-covariance W becomes W_{HV}.

Considering $(W_H - W_V)$ to be the 'z' axis of a right-handed 3-dimensional coordinate system, it can be shown that the x and y axes (i.e., $2|W_{HV}|\cos\phi$ and $2|W_{HV}|\sin\phi$) correspond to

$$2|W_{HV}|\cos\phi = W_{+45} - W_{-45} = U$$
$$2|W_{HV}|\sin\phi = W_{LHC} - W_{RHC} = V . \tag{9}$$

Returning to the decomposition matrices, and considering the two polarizations to be H and V, (5) become

$$2A = I - I_p = I(1 - p)$$
$$2B = I_p + Q$$
$$2C = I_p - Q \tag{10}$$

Considering Z_{DR} first, its value is usually determined from the ratio W_H / W_V. However, from (4), this corresponds to

$$\hat{Z}_{DR} = \frac{W_H}{W_V} = \frac{B + A}{C + A} = \frac{I + Q}{I - Q} . \tag{11}$$

This gives the correct result for Z_{DR} when the unpolarized power A is zero or negligibly small, but an increasingly biased result when an unpolarized component is present. This is because A is the same in both polarizations, while B and C are different in situations of interest. The correct formulation for differential reflectivity is the ratio of B and C by themselves, namely the ratio of the polarized powers. From (10), we have that

$$Z_{DR} = \frac{B}{C} = \frac{I_p + Q}{I_p - Q} = \frac{1 + Q/I_p}{1 - Q/I_p} . \tag{12}$$

The ratio Q/I_p is determined geometrically from Figure 8. The figure shows the polarization state P in the tilted 2α plane of Figure 2. The black and red semicircles represent the total power I, normalized to unity, and the polarized power $I_p = pI$. P has an H,V component Q and a polar angle relative to the H axis of 2α. The corresponding right triangle OPQ has base Q and hypotenuse I_p. From this, $Q/I_p = \cos(2\alpha)$, so that

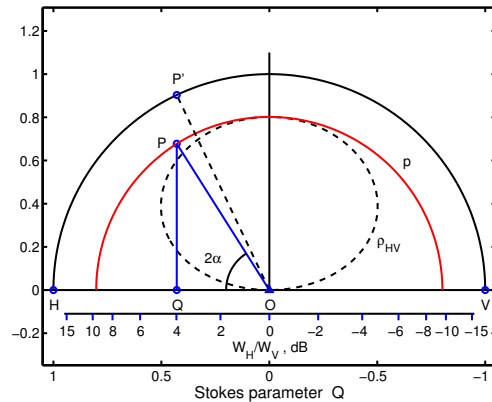$$Z_{DR} = \frac{1 + \cos(2\alpha)}{1 - \cos(2\alpha)} . \tag{13}$$

Figure 10. Geometric determination of Q/I_p for Z_{DR} measurements in the presence of an unpolarized component.
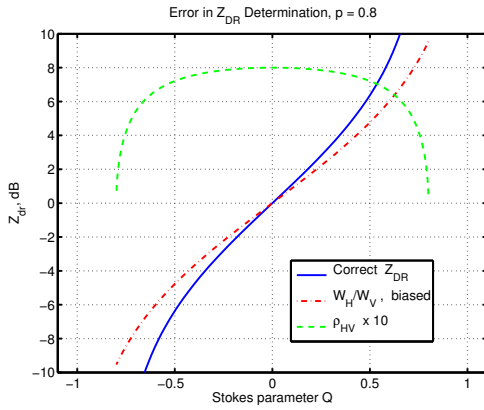
Figure 11. Error in Z_{DR} determination using W_H/W_V measurements in the presence of an unpolarized component (p = 0.8).

Figure 11 shows the difference between the actual values of Z_{DR} obtained from (12) or (13), and the biased values $\widehat{Z}_{DR}$ obtained from W_H/W_V (11). The results are for a degree of polarization $p = 0.8$ and are plotted vs. the normalized Stokes parameter Q, as in Figure 10. For a given actual value Z_{DR}, the W_H/W_V estimate is decreased in magnitude (toward unity, or 0 dB), owing to the addition of equal amounts of unpolarized power in both the numerator and denominator of (11). Stated the other way around, if $\widehat{Z}_{DR} = W_H/W_V$ is the calculated value of Z_{DR}, the actual value is larger in magnitude. The difference is less for smaller Z_{DR} magnitudes, and also for increased degrees of polarization, but is about 1.5 dB for actual Z_{DR} values of $\simeq 6$ dB and $p = 0.8$. The bias is therefore most important at larger Z_{DR} magnitudes and decreased degrees of polarization.

Similarly affected by the presence of an unpolarized component are the reflectivity factors Z_H and Z_V. Like Z_{DR}, their theoretical values also correspond to the polarized components of the measured powers W_H and W_V, namely to B and C. In particular, $B = kZ_H$, where k is the constant of proportionality. From the fact that $W_H = B + A$, $B = W_H - A = W_H - \frac{1}{2}(I - I_p)$. Thus,

$$kZ_H = W_H - \tfrac{1}{2}\left(I_{\text{unpolarized}}\right) \tag{14}$$
$$kZ_V = W_V - \tfrac{1}{2}\left(I_{\text{unpolarized}}\right) . \tag{15}$$

$I_{\text{unpolarized}}$ can be calculated either directly from the Stokes parameters or using the degree of polarization.

Finally, the fact that $D = W = \rho_{HV}e^{j\phi}$ is unaffected by the presence of an unpolarized component means that both ρ_{HV} and ϕ are correct as originally determined. However, as noted by Scott et al. (2001) and Galletti and Zrnic (2012), p and ρ_{HV} are related to each other by the general relation (Born and Wolf, 1975)

$$(1-p^2) = \left(\frac{\overline{W}_{\text{geom}}}{\overline{W}_{\text{arith}}}\right)^2 (1-\rho^2) , \tag{16}$$

where

$$\left(\frac{\overline{W}_{\text{geom}}}{\overline{W}_{\text{arith}}}\right)^2 = \frac{4}{\left(\frac{W_1}{W_2} + 2 + \frac{W_2}{W_1}\right)} = \frac{4}{\left(\sqrt{\frac{W_1}{W_2}} + \sqrt{\frac{W_2}{W_1}}\right)^2} . \tag{17}$$

The result is independent of basis. Solving for the degree of polarization gives p as a function of the polarization ratio W_1/W_2 and ρ:

$$p = \sqrt{1 - \frac{4(1-\rho^2)}{\left(\frac{W_1}{W_2} + 2 + \frac{W_2}{W_1}\right)}} . \tag{18}$$

The basic significance of the above is that p and ρ are not independent quantities. As described by Scott et al. (2001), randomly oriented scatterers fundamentally change p rather than ρ. Inversely, the change in ρ depends on the polarization ratio as well as p, as depicted by the dashed oval line in Figure 10. p directly detects the sphericity parameter g of randomly oriented and shaped particles, and therefore is the more fundamental physical quantity, as also concluded by Galletti and Zrnic (2012). Although p can be determined from (18), it is more directly and simply calculated from the Stokes parameters, as

$$p = \frac{I_p}{I} = \frac{\sqrt{Q^2 + U^2 + V^2}}{I} . \tag{19}$$

Galletti and Zrnic (2012) investigated the effect of depolarizing scatterers (i.e., scatterers that have non-zero off diagonal terms in the scattering matrix) on simultaneous H,V polarization measurements. They concluded that both ρ_{HV} and Z_{DR} measurements are biased by such scatterers, due to the off diagonal terms causing coupling between the two polarizations.

The above coupling does indeed occur but causes an unpolarized component in the backscattered signal. This results from the depolarizing particles having random shapes and/or orientations, or random orientation about a mean value. The basic analysis leading up to (4) at the beginning of this section shows that ρ_{HV} is not biased by the presence of an unpolarized component.

What is biased is the physical Z_{DR} value, when measured as the ratio W_H/W_V. The bias does not occur when Z_{DR} is determined as in (12) or (13). The basic reason for this is that simultaneous measurements directly detect and fully account for the presence of unpolarized components through the degree of polarization p.

The above is in contrast to alternating H and V transmissions, which indirectly sense an unpolarized component by incoherent LDR measurements and/or by pulse-pair ρ_{HV} measurements interpolated back to zero time lag, i.e., $\rho_{HV}(0)$. Both techniques have significant uncertainties in comparison to simultaneous measurements. For this reason and because there are no biases, simultaneous transmissions are the preferred mode of measurement.

Summary. The correct procedure for analyzing dual-polarization observations in an H,V basis is first to calculate the Stokes parameters from the covariance measurements, according to

$$\mathrm{I} = W_H + W_V$$
$$\mathrm{Q} = W_H - W_V$$
$$\mathrm{U} = 2|W_{HV}|\cos\phi_{HV}$$
$$\mathrm{V} = 2|W_{HV}|\sin\phi_{HV} \ . \tag{20}$$

Then calculate the polarized power I_p and degree of polarization p from

$$I_p = \sqrt{\mathrm{Q}^2 + \mathrm{U}^2 + \mathrm{V}^2} \tag{21}$$
$$p = \mathrm{I}_p/\mathrm{I} \ . \tag{22}$$

Calculate the H,V precipitation parameters Z_H, Z_V and Z_{DR} from

$$kZ_H = W_H - \tfrac{1}{2}(\mathrm{I} - \mathrm{I}_p) \tag{23}$$
$$kZ_V = W_V - \tfrac{1}{2}(\mathrm{I} - \mathrm{I}_p) \ , \tag{24}$$
$$Z_{\mathrm{DR}} = \frac{\mathrm{I}_p + \mathrm{Q}}{\mathrm{I}_p - \mathrm{Q}} \ , \tag{25}$$

and ρ_{HV} and ϕ from

$$\rho_{HV} = |W_{HV}| \tag{26}$$
$$\phi = \phi_{HV} \ . \tag{27}$$

Finally, display the precipitation variables of interest, including p and I_p, along with top ($-\mathrm{Q}$ vs. U), front (V vs. U), and side (V vs. $-\mathrm{Q}$) projection views of the polarization trajectory along the current or selected radial beam of the radar (or a 3-D rotatable view of unit Poincaré sphere and trajectory).

REFERENCES

V. N. Bringi and V. Chandrasekhar, Polarimetric Doppler Weather Radar. Principles and Applications. Cambridge, U.K.: Cambridge Univ. Press, 2001.

M. Born and E. Wolf, Principles of Optics: Electromagnetic Theory of Propagation, Interference and Diffraction of Light, 7th ed., Cambridge Univ. Press, 1999.

Galletti, M. and D. S. Zrnic, Degree of polarization at simultaneous transmit: Theoretical aspects, IEEE Geosci. and Remote Sensing Letts., 9, 383-387, May 2012.

Krehbiel, P., and R. Scott, A geometric approach to characterizing and interpreting dual-polarization radar meteorological observations, working document, 1999,2005.

Mott, H., Polarization in Antennas and Radar, J. Wiley, New York, 1986.

Ryzhkov, A., and D. S. Zrnic, Depolarization in ice crystals and its effect on radar polarimetric measurements, J. Atmos. Oceanic Technol., 24, 1256-1267, 2007.

Scott, R., Dual-polarization radar meteorology: A geometrical approach, Ph.D. Diss., New Mexico Institute of Mining and Technology, 129 pp., 1999 (available at http://lightning.nmt.edu/radar).

Scott, R., P. Krehbiel, and W. Rison, The use of simultaneous horizontal and vertical transmissions for dual-polarization radar meteorological observations, J. Atmos. and Oceanic Tech., 18, 629-648, 2001.

Scott, R., and P. Krehbiel, A geometric approach to characterizing and interpreting dual-polarization radar meteorological observations, paper 5B.1, 30th Conf./ Radar Meteorol., Munich, 2001 (available at http://lightning.nmt.edu/radar).

Scott, R., P. Krehbiel, and W. Rison, The use of simultaneous horizontal and vertical transmissions for dual-polarization radar meteorological observations, paper 5B.2, 30th Conf./ Radar Meteorol., Munich, 2001 (available at http://lightning.nmt.edu/radar).